

# Thermal Management and Interfacial Properties in High-Power GaN-Based Light-Emitting Diodes Employing Diamond-Added Sn-3 wt.%Ag-0.5 wt.%Cu Solder as a Die-Attach Material

CHIA-JU CHEN,<sup>1</sup> CHIH-MING CHEN,<sup>1,5</sup> RAY-HUA HORNG,<sup>2</sup>  
DONG-SING WUU,<sup>3</sup> and JHIH-SIN HONG<sup>4</sup>

1.—Department of Chemical Engineering, National Chung Hsing University, Taichung 402, Taiwan. 2.—Department of Electro-Optical Engineering, National Cheng Kung University, Tainan 701, Taiwan. 3.—Department of Materials Science and Engineering, National Chung Hsing University, Taichung 402, Taiwan. 4.—Institute of Precision Engineering, National Chung Hsing University, Taichung 402, Taiwan. 5.—e-mail: chenncm@nchu.edu.tw

The thermal management of high-power GaN-based light-emitting diodes (LEDs) soldered with Sn-3 wt.%Ag-0.5 wt.%Cu (SAC305) solder and diamond-added SAC305 solder was evaluated. Diamond addition was found to significantly reduce the surface temperature and total thermal resistance of the LEDs, revealing that diamond-added SAC305 solder is a promising die-attach material for high-power LED packaging. Interfacial reactions in the LED solder joints were also investigated. The thin Au wetting layer in the chip's backside metallization was rapidly consumed in the initial stage of reflow, forming an AuSn<sub>4</sub> phase at the interface. Subsequently, the AuSn<sub>4</sub> phase detached from the interface, leading to dewetting of the SAC305 solder from the LED chip. To avoid dewetting, a new backside metallization of LED chips should be developed for SAC305 solder.

**Key words:** Thermal resistance, diamond, die-attach materials, interfacial reaction, light-emitting diodes

## INTRODUCTION

In the packaging of conventional light-emitting diodes (LEDs), silver paste is commonly used as a die-attach material to bond the LED chip to a heat sink. A die-attach material acts not only as an adhesive but also as a heat dissipation path to remove the heat generated by the LED and transfer it to the heat sink. Recently, high-power GaN-based LEDs have attracted much attention and are considered candidates for next-generation general illumination applications due to their high luminous efficiency, long operating life, energy savings, and so forth.<sup>1</sup> However, a power saturation phenomenon<sup>2</sup> was often encountered in the operation of GaN-based LEDs packaged with silver paste when the current injection level was raised. This is

because the thermal conductivity of silver paste is poor and the heat generated from LEDs was not being efficiently dissipated, resulting in reduced conversion efficiency with increasing junction temperature. Therefore, development of new die-attach materials with high thermal conductivity for high-power LEDs is urgently required. Metallic solder materials, such as Au-20 wt.%Sn and Sn-Ag-Cu alloys, were proposed to replace the silver paste and have been introduced in LED packaging.<sup>3,4</sup>

Table I lists the thermal conductivities of die-attach materials currently used in LED packaging. The thermal conductivity of diamond is also listed for comparison. In general, metallic solder alloys exhibit better thermal conduction capability than epoxy and silver paste, while diamond possesses the highest thermal conductivity, being undoubtedly the best heat dissipation material.<sup>5-7</sup> Therefore, application of diamond in LED packaging is a promising strategy for improvement of thermal

(Received March 3, 2010; accepted August 2, 2010;  
published online September 2, 2010)

**Table I. Thermal conductivities of several common die-attach materials used for LED packaging**

Die-Attachment Material	Thermal Conductivity (W/m K)
Epoxy	0.2–0.3
Silver paste	2–25
Solder paste (Sn-3 wt.%Ag-0.5 wt.%Cu)	~60
Artificial diamond	~2000

management. In the present study, Sn-3 wt.%Ag-0.5 wt.%Cu (SAC305) solder, with microsized diamond particles added, was used as the die-attach material. Surface temperature and thermal resistance of the LEDs during current injection were measured and used to investigate the effectiveness of diamond addition for heat dissipation.

In contrast to conventional silver paste, LED packaging employing SAC305 solder must undergo a reflow process. In this reflow process, the temperature is raised above the melting point of the solder. Then, the solder melts and wets the backside metallization of the LED chip and the heat-sink metallization. Interfacial reactions between the solder and metallization take place, and chemical bonding joins the chip and the heat sink. Understanding the interfacial reactions at solder/metallization interfaces can help in the evaluation of bonding reliability. However, interfacial reactions in LED packaging employing SAC305 solder have rarely been studied.<sup>2</sup> Therefore, the other focus of this study is on the interfacial reactions in LED packaging.

## EXPERIMENTAL PROCEDURES

### Fabrication of LED Devices

Commercial LED chips (ES-CADBV45B; Epistar, Taiwan) and an Al-based heat sink (TTI9218M; I-Chiun, Taiwan) were used to prepare the samples. The dimensions of the LED chip and heat sink were 1 mm × 1 mm and 18.7 mm × 18.7 mm, respectively. The backside metallization of the LED chip is Ti/Al/Cr/Pt/Au, where Ti/Al serves as the adhesive/mirror layer, Cr is the barrier layer, and Pt/Au is the wetting layer (~1 μm). The metallization of the heat sink is a Cu/Sn bilayer, where a 1 μm to 2 μm Sn layer is deposited on a 30 μm Cu layer. Two types of die-attach materials were used: commercial SAC305 solder paste and diamond-added SAC305 solder paste. The diamond-added SAC305 solder paste was prepared by mixing the solder paste with microsized diamond particles using a planetary mixer and deaerator in a weight ratio of 10:1. Two different sizes, 1 μm to 10 μm and 10 μm to 20 μm, of diamond particles were used, as shown in Fig. 1. To fabricate an LED device, the LED chip was bonded to a heat sink using solder. First, patterned

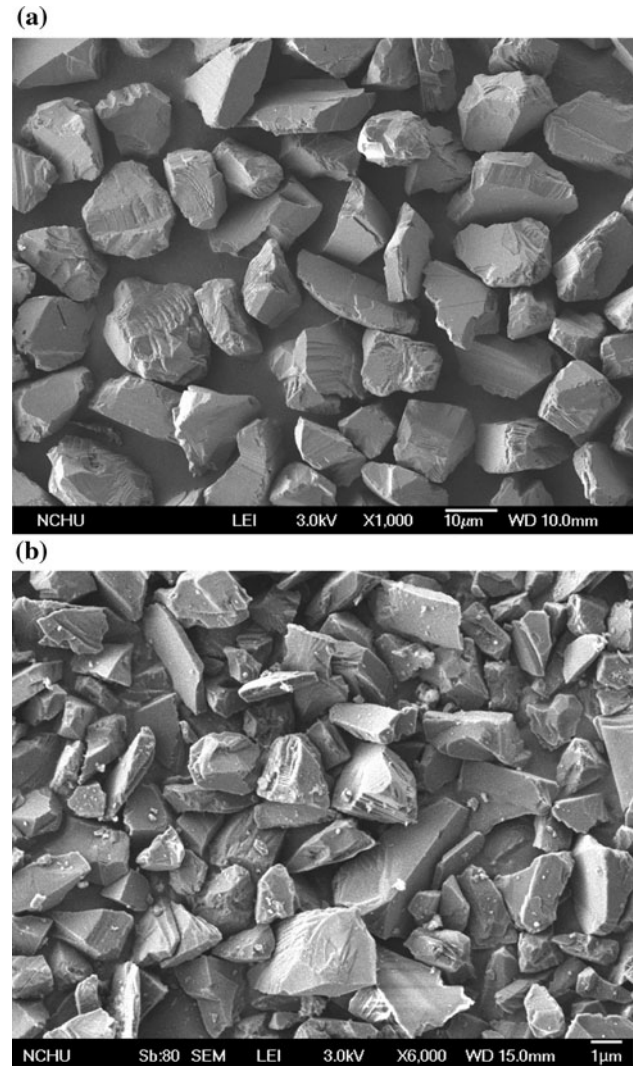


Fig. 1. SEM micrographs of diamond particles of different sizes: (a) 10 μm to 20 μm and (b) 1 μm to 10 μm.

solder paste (850 μm × 850 μm × 39 μm to 45 μm) was screen-printed onto the Cu/Sn metallization layer of a heat sink. Then, an LED chip was carefully placed on top of the solder paste. The heat sink with the attached LED chip was placed in a furnace to conduct the reflow process. The temperature was set at 250°C, and the time was 1 min. Another set of LED devices was fabricated using the above procedure but the die-attach material was conventional silver paste. This set of LED devices was used as a reference for comparison.

### Measurement of Surface Temperature and Thermal Resistance of LEDs During Current Injection

After reflow, the LED chips were wire-bonded to bonding pads on the heat sink to make an electrical connection. The as-fabricated LED device is shown schematically in Fig. 2. To measure the surface

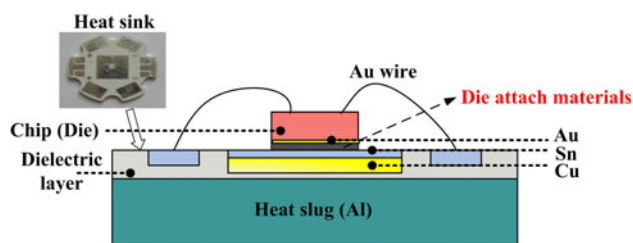


Fig. 2. Schematic of an LED device soldered with die-attach materials.

temperature of the LED chip in operation, a current of 350 mA was injected and the thermal infrared image was recorded after the LED had reached thermal equilibrium. The bottom of the heat sink was glued onto a cold plate using thermal grease. A T3ster thermal transient tester was used to measure the total thermal resistance of the LED based on thermal transient analysis.

### Investigation of Interfacial Reactions in the LED Devices

Two types of samples were fabricated. The first sample was prepared by screen-printing solder paste onto an LED chip. Then, reflow was conducted to investigate the interfacial reactions between the molten solder and the backside metallization of the LED chip. The reflow temperatures were 250°C and 350°C, and the time ranged from 30 s to 20 min. The preparation procedure of the second type of sample was the same as that described in the “Fabrication of LED Devices” section, being a chip/solder/heat sink sandwich-type structure. The reflow temperature and time were also the same as above. After the reaction, the samples were mounted and polished to expose the solder/metallization interfaces for cross-sectional examination using a scanning electron microscope (SEM). For clear observation, the samples were dipped into an etching solution (93% CH<sub>3</sub>OH + 5% HNO<sub>3</sub> + 2% HCl) to remove part of the solder. Compositional analysis of the reaction products was carried out using an energy-dispersive x-ray (EDX) spectrometer.

## RESULTS AND DISCUSSION

### Effects of Diamond Addition on the Surface Temperature Distribution and Thermal Resistance of LEDs

It is to be expected that the heat dissipation performance of a diamond-added solder paste can be enhanced by increasing the weight ratio of diamond particles to solder paste, due to the higher thermal conductivity of diamond. However, the viscosity of the solder paste also increases with increasing amounts of diamond, which results in difficulties in manufacturing and processing (screen-printing). Several weight ratios (solder paste to diamond) were tested, and the optimal (maximum) ratio for 1 μm to

10 μm and 10 μm to 20 μm diamond particles was about 10:1. Thus, the results reported in the present work were based on this ratio. Figure 3a–d shows the surface temperature distribution of the LED chips soldered with different die-attach materials at current injection of 350 mA. For the chips soldered with SAC305 solder, the chip surface temperature was very uniform and the maximum surface temperature was measured to be around 49°C, as seen in Fig. 3a. When small diamond particles (1 μm to 10 μm) at a weight ratio of 10:1 were added to the SAC305 solder, the chip surface temperature was uniform and the maximum temperature fell to around 42°C, as shown in Fig. 3b, revealing that the addition of small diamond particles indeed enhanced heat dissipation and that the chip temperature could be reduced by about 7°C. However, for the SAC305 solder with larger diamond particles (10 μm to 20 μm) at a weight ratio of 10:1, the chips exhibited inconsistent results. The surface temperature in some chips was successfully reduced to 44°C, as seen in Fig. 3c, but also increased to as high as 77°C in other chips, as seen in Fig. 3d.

To gain a better understanding of the heat dissipation behavior with different die-attach materials, the distributions of diamond particles in the solder joints of Fig. 3a–d were examined. Figure 3e–h shows cross-sectional SEM micrographs of the solder joints in Fig. 3a–d, respectively. Clearly, the black diamond particles in Fig. 3f and g were uniformly embedded in the solder matrix. The sunken regions in Fig. 3g were originally filled with diamond particles, but the diamond particles were removed due to mechanical polishing. This suggests that these diamond particles function as high thermal conductivity paths which can efficiently dissipate heat generated from the chips to the heat sink, leading to temperature reduction. However, the diamond particles in Fig. 3h severely aggregated toward the chip side, and a continuous gap was found along the interface. Because this gap is a very poor thermal conductivity path, the chip temperature increased. Another interesting phenomenon to investigate was the tendency of large diamond particles to aggregate at the chip side while small diamond particles did not. A plausible explanation takes into account the sizes of the diamond particles. During reflow, the solder paste melted and the diamond particles might float upward due to their lower density (3.5 g/cm<sup>3</sup>) as compared with the SAC305 solder (7.4 g/cm<sup>3</sup>). The buoyancy of large diamond particles in molten solder is bigger because they have larger volume. As a result, large diamond particles might easily float upward and aggregate at the chip side in a shorter time (less than 1 min, the reflow time). In contrast, smaller diamond particles could be frozen in the solder matrix due to insignificant buoyancy. Based on these results, the recommended size of diamond particles is less than 10 μm. Figure 4 compares the cumulative structure functions of the LEDs presented in Fig. 3. The total

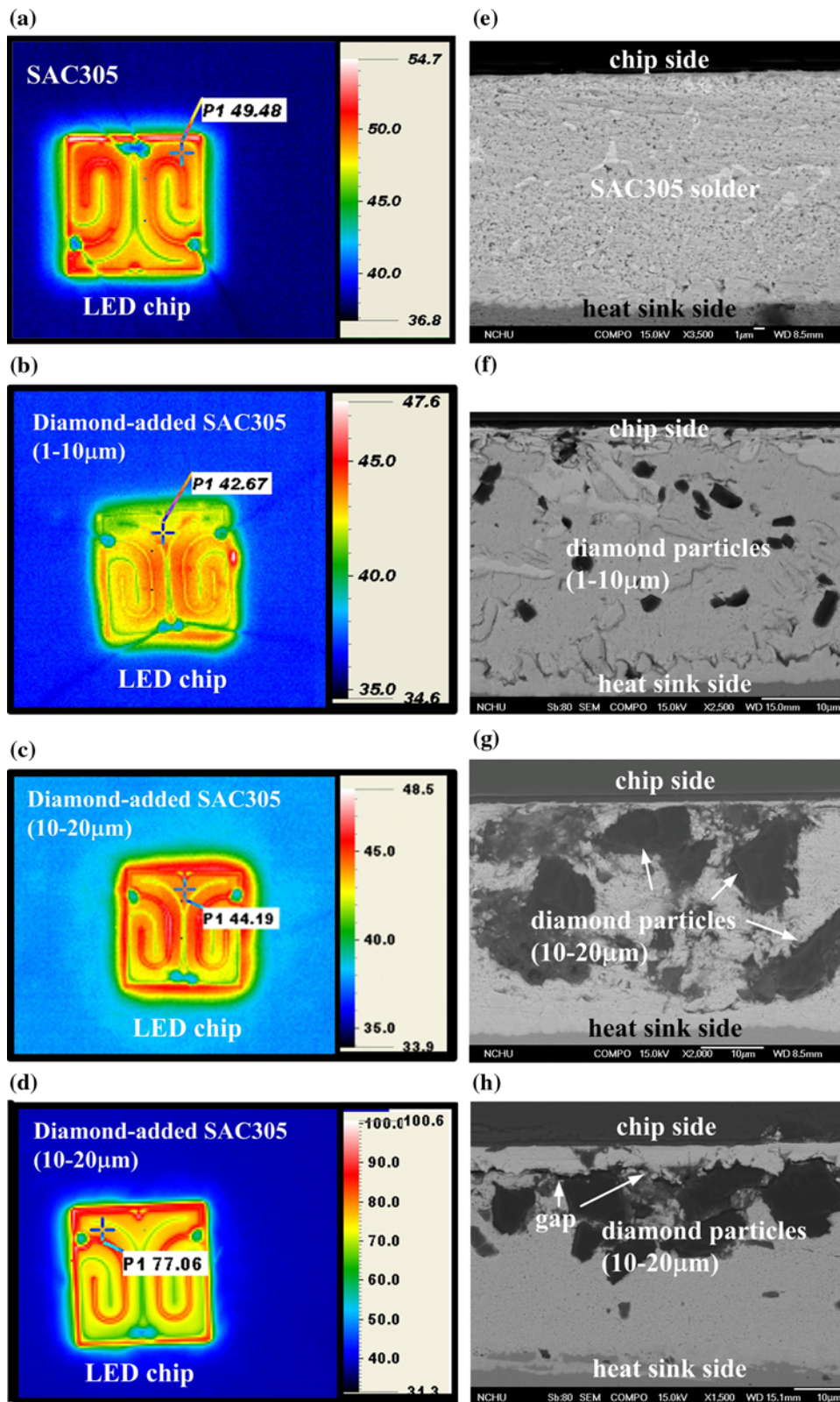


Fig. 3. Surface temperature distribution and cross-sectional SEM micrographs of LED devices soldered with different die-attach materials. The injection current is 350 mA.

thermal resistances of the LEDs in Fig. 3a–d are 14.3 K/W, 11.1 K/W, 13.2 K/W, and 80 K/W, respectively, consistent with the temperature

distribution trend on the chip surface. Obviously, the total thermal resistance of an LED device can be reduced by using diamond-added SAC305 solder,

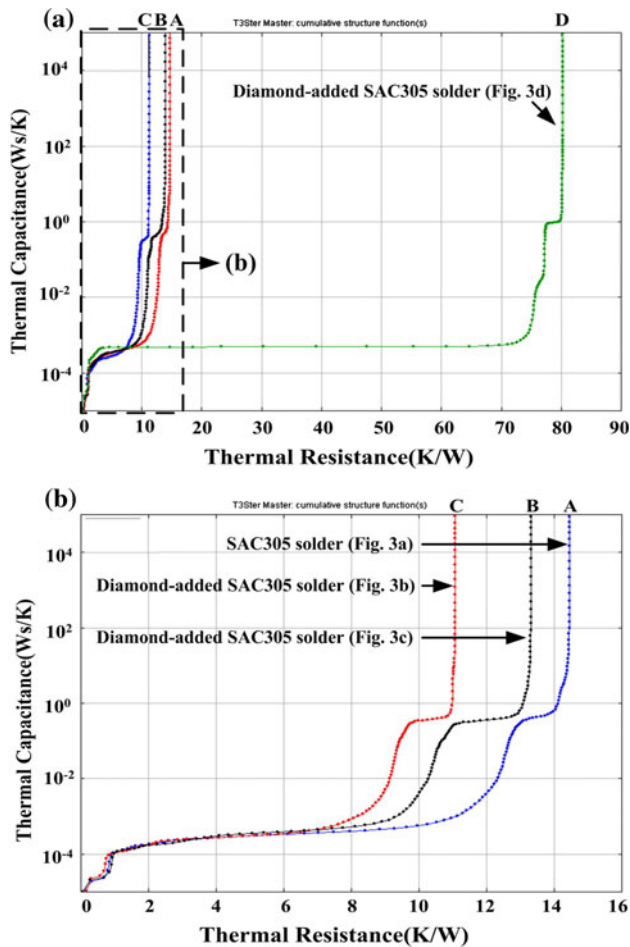


Fig. 4. Cumulative structure functions of the LED devices depicted in Fig. 3. The total thermal resistances of the LED devices in Fig. 3a–d are 14.3 K/W, 11.1 K/W, 13.2 K/W, and 80 K/W, respectively.

indicating that the addition of diamond is indeed a useful strategy for improving thermal management of LEDs.

The above analyses were also performed on the LED devices soldered with silver paste, and the results are shown in Fig. 5a–c, showing the surface temperature distribution, a cross-sectional SEM micrograph, and the cumulative structure function, respectively. It was found that both the maximum surface temperature of the LED chip ( $\sim 57^\circ\text{C}$ ) and the total thermal resistance ( $\sim 37.5$  K/W) were higher than those for chips soldered with pure SAC305 and diamond-added SAC305 solders, indicating that the heat dissipation performance of SAC305 solder is better than that of conventional silver paste.

Light output power is also a key performance metric of an LED and strongly depends upon carrier confinement in quantum wells.<sup>8</sup> As the chip temperature increases, carrier confinement in quantum wells becomes less efficient, leading to degradation in light output performance. Therefore, reducing the chip surface temperature is beneficial for

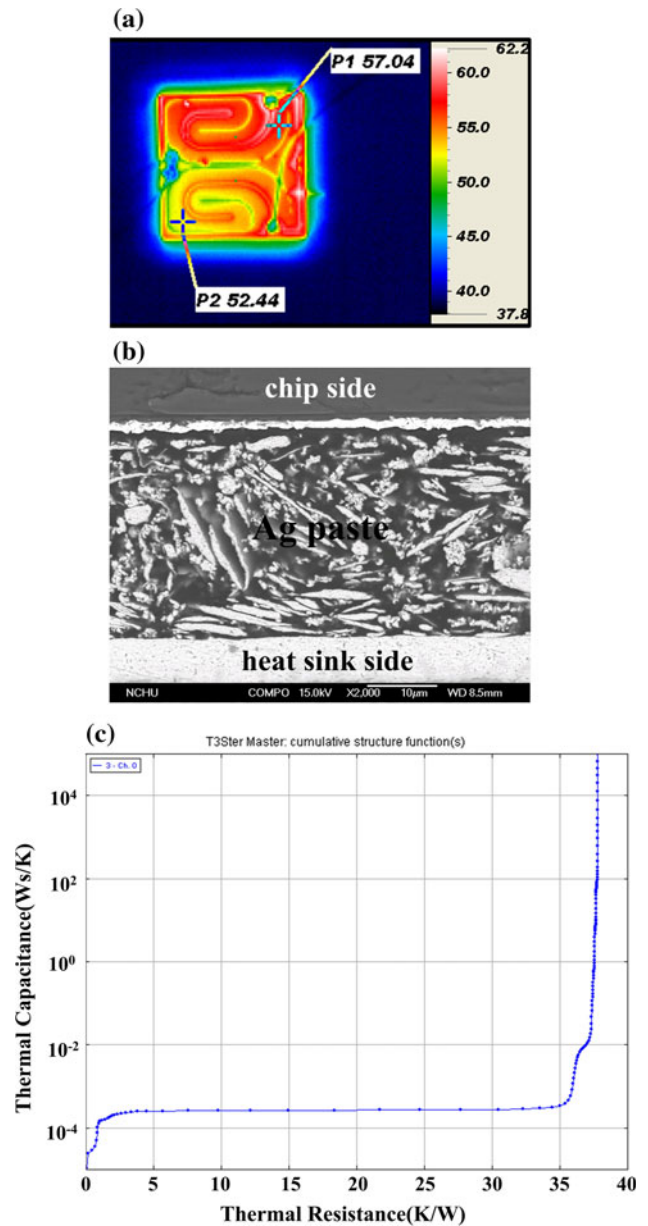


Fig. 5. (a) Surface temperature distribution, (b) cross-sectional SEM micrograph, and (c) cumulative structure function of a LED device soldered with silver paste. The injection current is 350 mA.

achieving better output power. Based on the above results, we can conclude that the addition of diamond particles to the solder die-attach material is a successful strategy for improvement of light output performance, due to reduced chip temperature.

### Interfacial Reactions in the LED Devices Soldered with SAC305

Although two types of die-attach materials, SAC305 and diamond-added SAC305, were prepared in the present work, the study of interfacial reactions focused only on the LEDs soldered with SAC305. The interfacial reaction at the LED joints soldered with diamond-added SAC305 is expected to

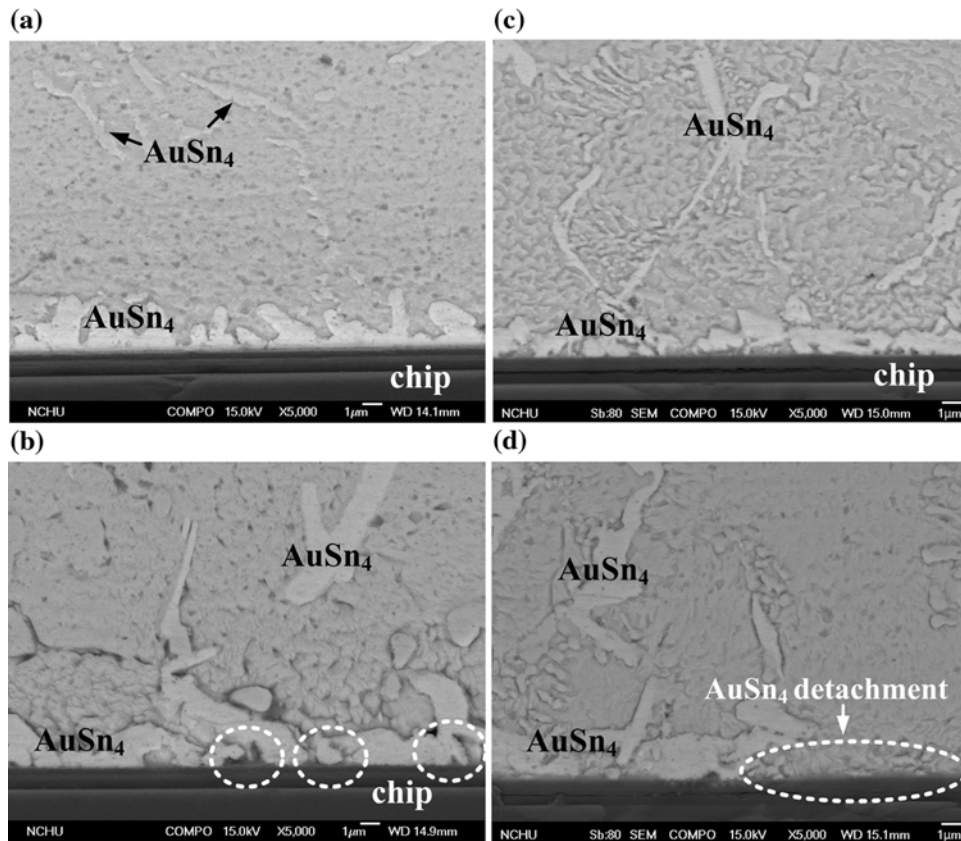


Fig. 6. Cross-sectional SEM micrographs of the joint interface in the LED chip/solder samples after reflow at 250°C for (a) 1 min, (b) 3 min, (c) 10 min, and (d) 20 min.

be very similar to that using SAC305, because diamond is an inert material at the reflow temperature and does not participate in the reactions. Figure 6 shows a series of SEM micrographs of the joint interfaces in the LED chip/solder samples after reflow at 250°C for different times. It was found that the thin Au layer of the chip's backside metallization was completely consumed, and an irregular layer was formed at the interface after 1 min of reflow, as seen in Fig. 6a. EDX analysis revealed that this new layer had a composition of 19.21 wt.%Au-80.79 wt.%Sn, indicating that it is the AuSn<sub>4</sub> phase. After 3 min of reflow, as seen in Fig. 6b, this AuSn<sub>4</sub> phase became more irregular and, at some interfacial regions, as marked by circles, the AuSn<sub>4</sub> phase detached from the backside Cr metallization. This detachment phenomenon was more significant after reflow for 10 min, as shown in Fig. 6c. After reflow for 20 min, a portion of the continuous AuSn<sub>4</sub> layer detached and the solder contacted the Cr layer directly, as seen in Fig. 6d. It is well known that Sn-based solder exhibits poor wettability on Cr,<sup>9</sup> so direct contact of the SAC305 solder with Cr is likely to lead to dewetting.

An obvious dewetting phenomenon can be observed in Fig. 7a, where reflow was conducted at 350°C for 10 min. The solder formed a cap on the

LED chip after reflow, and dewetting was observed at the cap rim. The magnified micrograph in Fig. 7b shows that the AuSn<sub>4</sub> layer near the dewetting region detached from the interface in large amounts. Significant AuSn<sub>4</sub> detachment was also observed elsewhere in this sample, as seen in Fig. 7c. Compared with Fig. 6d, the AuSn<sub>4</sub> layer in Fig. 7c detached at a faster rate, indicating that raising the reflow temperature would accelerate the AuSn<sub>4</sub> detachment rate and degrade the wettability of SAC305 solder on conventional backside metallization. The enhanced AuSn<sub>4</sub> detachment phenomenon is attributable to the faster interfacial reaction between the solder and Au at elevated temperatures. Once the Au layer is completely consumed to form the AuSn<sub>4</sub> phase, the solder/Au interfacial reaction ceases and a ripening reaction begins to dominate. The ripening reaction increases the AuSn<sub>4</sub> grain size but decreases the number of grains. Simultaneously, the contact area between AuSn<sub>4</sub> and the residual metallization (Cr) decreased, resulting in direct contact of the solder with the residual metallization (Cr). If the wettability of the solder on the residual metallization is poor, dewetting is very likely to occur. The detachment of the interfacial compounds and dewetting phenomena are described in detail elsewhere.<sup>10–12</sup>

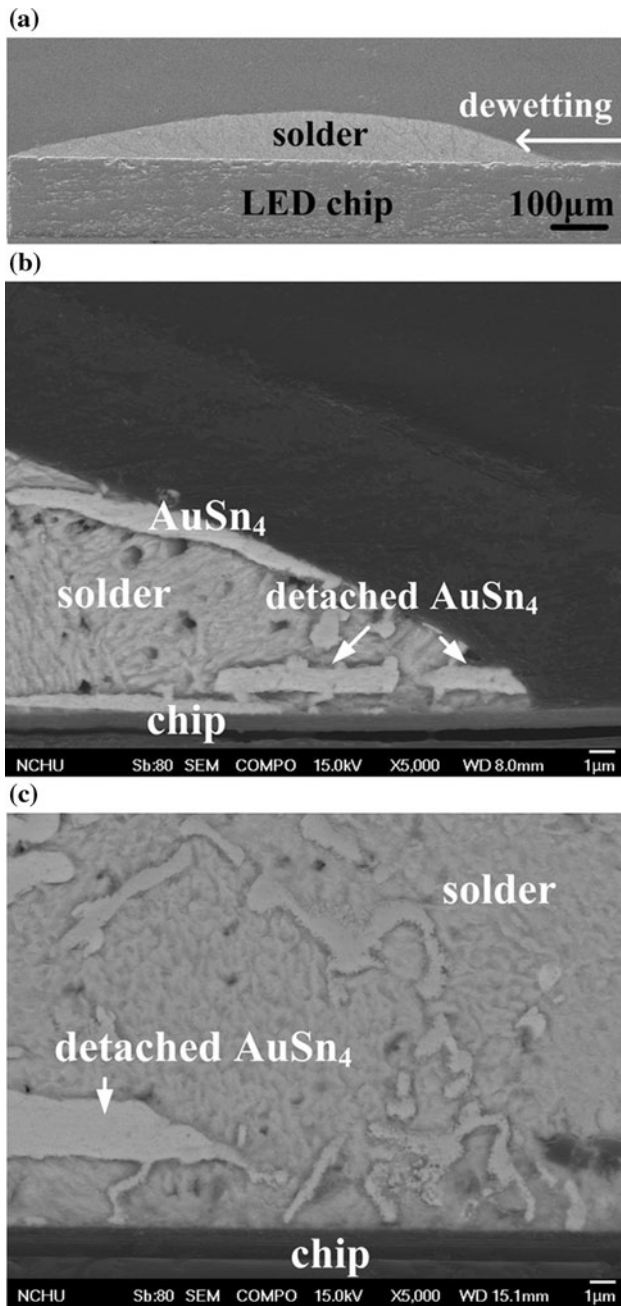


Fig. 7. Cross-sectional SEM micrographs of the joint interface in the LED chip/solder samples after reflow at 350°C for 10 min.

It has been proposed that a strategy for inhibiting the detachment of interfacial compounds and solder dewetting is to thicken the wetting metallization, so that the wetting metallization would not be completely consumed during the typical reflow time and the reaction compounds could still contact with the wetting metallization.<sup>13</sup> Therefore, thickening the Au layer may be a solution for LED packaging using SAC305 solder as a die-attach material. However, this is not practical due to the cost of Au. Therefore, it is necessary to develop an alternative wetting layer for LED packaging using SAC305 solder.

Cross-sectional SEM micrographs of the joint interfaces in the LED chip/solder/heat sink samples are shown in Fig. 8. Compared with the LED chip/solder sample, the LED chip/solder/heat sink sample is a commercial LED packaging with two joint interfaces for observation of interfacial reactions. One is at the chip side, the Au/solder interface, and the other at the heat-sink side, the solder/Cu interface. So, this can be seen as a sandwich-type Au/solder/Cu structure with very limited Au (1  $\mu\text{m}$  thick) and abundant Cu (30  $\mu\text{m}$  thick). After 1 min of reflow, two reaction products were found in the sample, as seen in Fig. 8a. According to the results of compositional analysis, the reaction product formed at the chip side is the (Au,Pt,Cu)Sn<sub>4</sub> phase (12.2 wt.%Cu-8.3 wt.%Au-3.19 wt.%Pt-76.31 wt.%Sn). At the heat-sink side, the phase is (Cu,Au)<sub>6</sub>Sn<sub>5</sub> (48.51 wt.%Cu-6.87 wt.%Au-44.62 wt.%Sn). The (Au,Pt,Cu)Sn<sub>4</sub> phase possesses the crystal structure of  $\eta$ -AuSn<sub>4</sub>, but some of the Au atoms are substituted by Pt and Cu atoms. The Cu source is the Cu metallization on the heat sink. During reflow, the molten solder dissolved part of the Cu metallization. The dissolved Cu atoms diffused upward into the chip side and participated in (Au,Pt,Cu)Sn<sub>4</sub> formation. Similarly, the molten solder also dissolved Au from the chip side, and the dissolved Au atoms crossed the molten solder joint to participate in the formation of (Cu,Au)<sub>6</sub>Sn<sub>5</sub> at the opposite side by the heat sink. Similar cross-interaction results between two opposite solder joint interfaces were also reported for the Au/Sn/Cu system.<sup>14</sup> There were some needle-like phases dispersed in the solder matrix that were identified as the AuSn<sub>4</sub> phase.

Upon increasing the reflow time, the (Cu,Au)<sub>6</sub>Sn<sub>5</sub> phase at the heat-sink side grew thicker, but the (Au,Pt,Cu)Sn<sub>4</sub> phase gradually detached from the upper interface. A comparison of Figs. 6 and 8 reveals that the AuSn<sub>4</sub> phase in the LED chip/solder/heat sink samples detached at a faster rate. The entire (Au,Pt,Cu)Sn<sub>4</sub> phase detached from the interface after 20 min of reflow, as displayed in Fig. 8d. Compositional analysis did not detect the existence of Au at the chip-side interface. The faster detachment rate of the (Au,Pt,Cu)Sn<sub>4</sub> phase may be a result of cross-interaction between two opposite interfacial reactions. When the dissolved Au atoms diffused to the opposite interface and were trapped by the (Cu,Au)<sub>6</sub>Sn<sub>5</sub> phase, the concentration of Au in the molten solder decreased, creating a concentration difference for continuous Au dissolution. Consequently, the Au layer was consumed at a faster rate, which accelerated detachment. Faster Au consumption due to cross-interaction between the two opposite interfacial reactions was also observed in the Au/Sn/Cu system.<sup>14</sup> As mentioned above, (Au,Pt,Cu)Sn<sub>4</sub> detachment might lead to dewetting of the solder from Cr. Dewetting phenomenon in the LED chip/solder/heat sink samples could be observed as early as 3 min into reflow, as seen in Fig. 9.

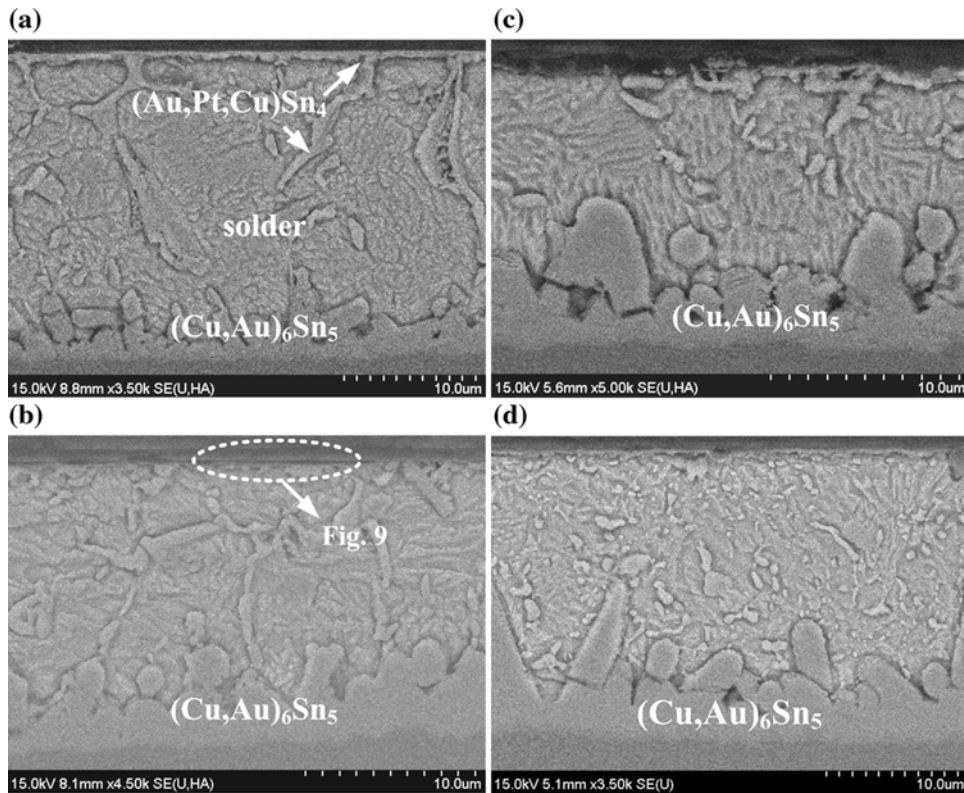


Fig. 8. Cross-sectional SEM micrographs of the joint interfaces in the LED chip/solder/heat sink samples after reflow at 250°C for (a) 1 min, (b) 3 min, (c) 10 min, and (d) 20 min.

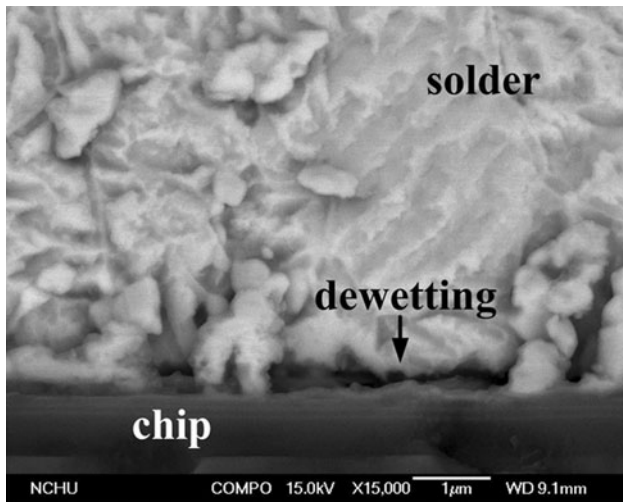


Fig. 9. Magnified cross-sectional SEM micrograph of the chip/solder interface in Fig. 8b.

### CONCLUSIONS

The addition of diamond to SAC305 solder is a successful strategy for improving the thermal management of high-power LEDs. Compared with conventional silver paste and SAC305 solder, use of diamond-added SAC305 solder, where the size of the diamond particles is about 1  $\mu\text{m}$  to 10  $\mu\text{m}$  and the weight ratio of solder to diamond is 10:1, can

reduce the surface temperature of the chip and the total thermal resistance of LED devices. The results of interfacial reactions in the LED solder joints revealed that the thin Au wetting layer of the chip's backside metallization was totally and rapidly consumed by the molten solder. The  $\text{AuSn}_4$  phase then formed at the chip-side interface via a reaction between the solder and Au. Absence of the Au wetting layer was found to lead to detachment of the  $\text{AuSn}_4$  phase and dewetting of the solder from the residual metallization. Because solder dewetting degrades the mechanical properties and heat dissipation performance of the joint, designing a more appropriate wetting layer appears necessary for high-power LEDs employing SAC305 solder as a die-attach material.

### ACKNOWLEDGEMENTS

This work was supported by the National Science Council and Ministry of Economic Affairs, Taiwan, ROC, with Grant Nos. NSC 96-2218-E-007-012 and 97-EC-17-A-07-S1-097, respectively. This work is supported in part by the Ministry of Education, Taiwan, ROC under the ATU plan.

### REFERENCES

1. M. Arik, J. Petroski, and S. Weaver, *Inter Soc. Conf. on Thermal Phenomena* (2004), p. 64.
2. H.H. Kim, S.H. Choi, S.H. Shin, Y.K. Lee, S.M. Choi, and S. Yi, *Microelectron. Reliab.* 48, 445 (2008).



3. F.P. McCluskey, M. Dash, Z. Wang, and D. Huff, *Microelectron. Reliab.* 46, 1910 (2006).
4. J.W. Park, Y.B. Yoon, S.H. Shin, and S.H. Choi, *Mater. Sci. Eng. A* 441, 357 (2006).
5. S.L. Shinde and J.S. Goela, *High Thermal Conductivity Materials* (New York: Springer, 2006).
6. P.H. Chen, C.L. Lin, Y.K. Liu, T.Y. Chung, and C.Y. Liu, *IEEE Photonics Technol. Lett.* 20, 10 (2008).
7. P. Hui and H.S. Tan, *J. Appl. Phys.* 75, 748 (1994).
8. N. Narendran and Y. Gu, *IEEE OSA J. Disp. Technol.* 1, 1 (2005).
9. S.Y. Jang, J. Wolf, O. Ehrmann, H. Gloor, H. Reichl, and K.W. Paik, *IEEE Trans. Electron. Packag. Manuf.* 25, 193 (2002).
10. H.K. Kim and K.N. Tu, *Appl. Phys. Lett.* 68, 16 (1996).
11. D.W. Zheng, Z.Y. Jia, C.Y. Liu, W. Wen, and K.N. Tu, *J. Mater. Res.* 13, 5 (1998).
12. K.N. Tu and K. Zeng, *Mater. Sci. Eng.* 34, 58 (2001).
13. M.S. Shin and Y.H. Kim, *J. Electron. Mater.* 32, 1448 (2003).
14. Y.W. Yen, H.W. Tseng, K. Zeng, S.J. Wang, and C.Y. Liu, *J. Electron. Mater.* 38, 2257 (2009).